Coupled Translation−Rotation Eigenstates of H_2, HD, and D_2 in the Large Cage of Structure II Clathrate Hydrate: Comparison with the Small Cage and Rotational Raman Spectroscopy†

Minzhong Xu, Francesco Sebastianelli, and Zlatko Bačić*

Department of Chemistry, New York University, New York, New York 10003

Received: March 3, 2009; Revised Manuscript Received: April 13, 2009

We report fully coupled quantum five-dimensional calculations of the translation−rotation (T-R) energy levels of one H_2, HD, and D_2 molecule confined inside the large hexakaidecahedral ($5^{12}6^4$) cage of the structure II clathrate hydrate. Highly converged T-R eigenstates have been obtained for excitation energies beyond the $j = 2$ rotational levels of the guest molecules, in order to allow comparison with the recent Raman spectroscopic measurements. The translationally excited T-R states are assigned with the quantum numbers n and l of the 3D isotropic harmonic oscillator. However, the translational excitations are not harmonic, since the level energies depend not only on n but also on l. For $l > 1$, the T-R levels having the same n,l values are split into groups of almost degenerate levels. The splitting patterns follow the predictions of group theory for the environment of T_d symmetry, which is created by the configuration of the oxygen atoms of the large cage. The $2j + 1$ degeneracy of the $j = 1$ and 2 rotational levels of the encapsulated hydrogen molecule is lifted entirely by the angular anisotropy of the H_2−cage interaction potential. The patterns and magnitudes of the $j = 1$, 2 rotational level splittings, and the energies of the sublevels, in the large cage are virtually identical with those calculated for the small cage. This is in agreement with, and sheds light on, the observation that the $S_0(0)$ ($j = 0 \rightarrow 2$) bands in the rotational Raman spectra measured for simple H_2 hydrate and the binary hydrate of H_2 with tetrahydrofuran are remarkably similar with respect to their frequencies, widths, shapes, and internal structure, when the H_2 occupancy of the large cage of simple H_2 hydrate is low.

I. Introduction

Clathrate hydrates are inclusion compounds where a variety of small molecules are trapped inside closely packed polyhedral cavities within the crystalline host lattice formed by hydrogen-bonded water molecules.[1−3] For a long time it was widely considered that hydrogen molecules are too small, and interact too weakly with the framework water molecules, to stabilize the clathrate structure. However, this view underwent a complete revision in the past decade, during which it has been demonstrated that molecular hydrogen does form clathrate hydrates.[4,5] Simple hydrogen hydrates, where hydrogen molecules are the sole guests, have the classical structure II (sII)[1,2] whose unit cell is cubic, with 136 water molecules organized in the hydrogen-bonded framework comprised of two types of cages: sixteen dodecahedral (5^{12}), or "small" cages, with 12 pentagonal faces, and eight hexakaidecahedral ($5^{12}6^4$), or "large" cages, having 12 pentagonal and 4 hexagonal faces. Up to four hydrogen molecules can be trapped in the large cage and only one in the small cage.[6] Hydrogen hydrates have attracted a great deal of attention because of their potential as environmentally friendly and efficient materials for hydrogen storage.[1,2,7−9] One of the shortcomings of simple hydrogen hydrates (where H_2 is the only guest molecule) is the high pressure of about 200 MPa at 250 K required for their synthesis, and considerable effort has been aimed at removing or lessening this obstacle. It has been shown that in the presence of the second, larger guest molecule such as tetrahydrofuran (THF), the sII hydrogen hydrate can be stabilized at the much lower formation pressure of 5 MPa at 280 K.[10,11] However, the price for this is the reduced hydrogen storage capacity, since in the binary THF + H_2 hydrate the THF molecules occupy all the large cages, leaving only the small clathrate cages for storing the hydrogen molecules, one H_2 per cage. In addition, molecular hydrogen can be trapped within binary structure I (sI)[12] and structure H (sH) hydrates,[13] in the presence of suitable promoter molecules.

Besides their promise as hydrogen storage materials, hydrogen hydrates provide an outstanding opportunity for studying the quantum dynamical effects arising from the nanoscale confinement of light rotors in the small and large cages. The confinement results in the quantization of the translational degrees of freedom of the guest molecules, in addition to their quantized rotational states. Since the hydrogen molecules are light and have large rotational constants, their discrete translational and rotational states are well separated in energy. The translation−rotation (T-R) energy level structure of the trapped homonuclear isotopomers H_2 and D_2 is made even sparser by the symmetry constraints on their total wave functions: p-H_2, with the total nuclear spin $I = 0$, and o-D_2 with $I = 0$ or 2, can exist in even-j rotational states only ($j = 0, 2, 4, \cdots$), while o-H_2 and p-D_2, both with $I = 1$, have exclusively odd-j rotational states ($j = 1, 3, 5, \cdots$). Finally, the zero-point energy (ZPE) of the coupled T-R motions is substantial relative to the well depth of the interaction potential. Due to these large quantum effects, the hydrogen molecules encapsulated inside the clathrate cages constitute a highly quantum mechanical system, especially at the low temperatures at which the hydrogen hydrates are prepared and at which most of the experiments on them are performed. Therefore, reliable theoretical predictions regarding

† Part of the "Robert Benny Gerber Festschrift".

* Author to whom correspondence should be addressed. E-mail: zlatko.bacic@nyu.edu.

10.1021/jp901951k CCC: $40.75
Published on Web 05/04/2009

the spectroscopy and the energetics of hydrogen hydrates at low temperatures, as well as the number of trapped hydrogen molecules and their spatial distribution inside the small and large clathrate cages, can be made only by resorting to a fully quantum mechanical treatment, solving the multidimensional Schrödinger equation for the coupled T-R motions of the guest hydrogen molecules.

Nevertheless, prior to our recent work outlined below, the few theoretical studies of the hydrogen hydrates which attempted to include some quantum effects did that in a variety of highly approximate and simplified ways,[14−16] precluding a realistic description of the T-R energy level structure of the encapsulated hydrogen molecule(s). Over the past several years, in a series of papers we investigated rigorously for the first time the quantum T-R dynamics of hydrogen molecules confined in the cavities of the sII clathrate hydrate.[17−22] Our theoretical approach treats the three translational and the two rotational degrees of freedom of a confined hydrogen molecule explicitly, as fully coupled, without any dynamical approximation, and the clathrate cages are assumed to be rigid, with their geometries taken from the X-ray diffraction experiments.[23] For a single hydrogen molecule in the small cage,[17,20,21] the salient features of the T-R eigenstates revealed by the quantum 5D calculations include the splitting of the translational fundamental, the negative anharmonicity of the translational excitations, and complete removal of the $2j + 1$ degeneracy of the $j = 1$ and 2 rotational levels, with the latter split into a distinctive quintuplet pattern.[20,21] The cause of the splittings of both the translational and the rotational excitations of the hydrogen molecule are the anisotropies of the cage environment, the former with respect to the translational motion of the center of mass (cm) of the guest molecule, and the latter with respect to its angular orientation within the cage. For a hydrogen molecule in the small cage, our results concerning the splitting of the translational fundamental and the $j = 1$ triplet of H_2 and HD have been corroborated by the inelastic neutron scattering (INS) studies of THF + H_2 and THF + HD hydrates;[24,25] the predicted lifting of the 5-fold degeneracy of the $j = 2$ level of H_2, HD, and D_2 has been observed in the rotational Raman spectra of THF + H_2,[26,27] THF + HD,[26] and THF + D_2 hydrates.[27] The agreement between theory and the experimental data about the T-R excitations in the small cage is qualitative for the quantum 5D calculations[17,20] performed on the pairwise additive H_2−cage potential energy surface (PES) designated as PA-D,[21] constructed by using the ab initio 5D PES of the H_2−H_2O van der Waals complex;[28] the accord is much better, near-quantitative for the results of our latest study of H_2, HD, and D_2, inside the small cage,[21] which utilized the H_2−cage interaction potential by Alavi and co-workers.[29] This 5D PES, also pairwise additive, is based on the extended simple point charge (SPC/E) effective H_2O−H_2O pair potential of Berendsen et al.,[30] and has been referred to by us as SPC/E.

The T-R dynamics of hydrogen molecules in the *large* cage has not been investigated at a comparable level of detail. We have performed the diffusion Monte Carlo (DMC) calculations of the ground state properties, energetics, and spatial distributions, of small $(p\text{-}H_2)_n$ and $(o\text{-}D_2)_n$ clusters, $n = 1-5$, in the large cage.[22] The calculations showed that the rapid increase of cluster ZPE with n is the main factor limiting the large cage occupancy to at most four H_2 or D_2 molecules, in agreement with the neutron diffraction measurements[6] made below 70 K and at ambient pressure. Moreover, the DMC-calculated vibrationally averaged tetrahedral arrangement of the four D_2 molecules inside the large cage agrees quantitatively with the low-temperature experimental data[6] in terms of their mean distance from the cage center, the D_2−D_2 separation, and the particular orientation of the $(D_2)_4$ cluster relative to the cage framework. However, scant information was available about the T-R excitations in the large cage, from either experiment or theory. The molecular hydrogen rotons $S_0(0)$, $S_0(1)$, and $S_0(2)$, corresponding to the purely rotational $\Delta j = 2$ transitions out of the states $j = 0$, 1, and 2, respectively, of H_2 have been observed at low resolution in the Raman spectra of the simple H_2 hydrate,[5] at frequencies close to those for H_2 in the gas phase, suggesting nearly free rotation of the guest molecules.

Very recently, the rotational $S_0(0)$ and $S_0(1)$ bands for simple H_2 hydrate, and also THF + H_2 hydrate, have been reported with much better resolution.[26,27] The $S_0(0)$ band shows internal structure, which is particularly well resolved in ref 27. The top of the band is split into three distinguishable peaks separated by about 3.5 cm^{-1}. In contrast, the $S_0(1)$ band appears as a single broad peak with no resolvable splitting. For low H_2 loading of the large cage, less than three molecules, both the $S_0(0)$ and $S_0(1)$ bands of simple H_2 hydrate bear a close similarity to the rotational Raman bands of THF + H_2 hydrate. The structure at the top of $S_0(0)$ band for simple H_2 hydrate remains essentially unchanged as the H_2 content of the large cage is varied. However, the bases of both the $S_0(0)$ and $S_0(1)$ bands broaden substantially with increasing H_2 occupancy.[27] This can be caused by the greater angular, orientational anisotropy of the interaction potential in the large cage when three or four H_2 molecules are present, and also by the dynamical coupling between their T-R motions.

The new higher resolution Raman spectroscopic data about the $S_0(0)$ band of simple H_2 hydrate, and in particular how its structure evolves with the increasing large-cavity H_2 content, will be the subject of our future theoretical investigations. But the essential prerequisite for such studies is to have quantitative information about the higher lying T-R eigenstates of a single hydrogen molecule in the large cage, which would include the $j = 2$ rotational manifold. This has motivated us to undertake rigorous quantum 5D calculations of the T-R energy levels of one H_2, HD, and D_2 molecule inside the large cage, up to the $j = 2$ rotational levels of the guest molecules, which are presented in this paper. Such calculations are considerably more demanding computationally than for the small cage. The fundamental and higher translational excitations have much lower frequencies in the large cage than in the small cage, giving rise to a considerably higher density of states in the former. Consequently, there are many more highly translationally excited ($j = 0$) energy levels below the $j = 2$ quintuplet of p-H_2 in the large cage than is the case in the small cage, so that a much larger basis is needed to get converged results. Our only study to date that addressed the T-R excitations in the large cage[19] was limited to just the lowest three excited translational states of H_2, and the PA-D H_2−cage PES was used, which, as we have established in the meantime, does not have the desired high level of quantitative accuracy. The results reported in this paper were obtained on the SPC/E PES, which has been demonstrated to provide a significantly more accurate representation of the H_2−cage interactions.[21,22] The computed T-R eigenstates are analyzed carefully, and quantum numbers are assigned to the states with up to three quanta in the translational mode. Extensive comparison is made with the T-R energy level structure determined for H_2, HD, and D_2 in the small cage,[21] as well as with the recent Raman spectroscopic measurements.

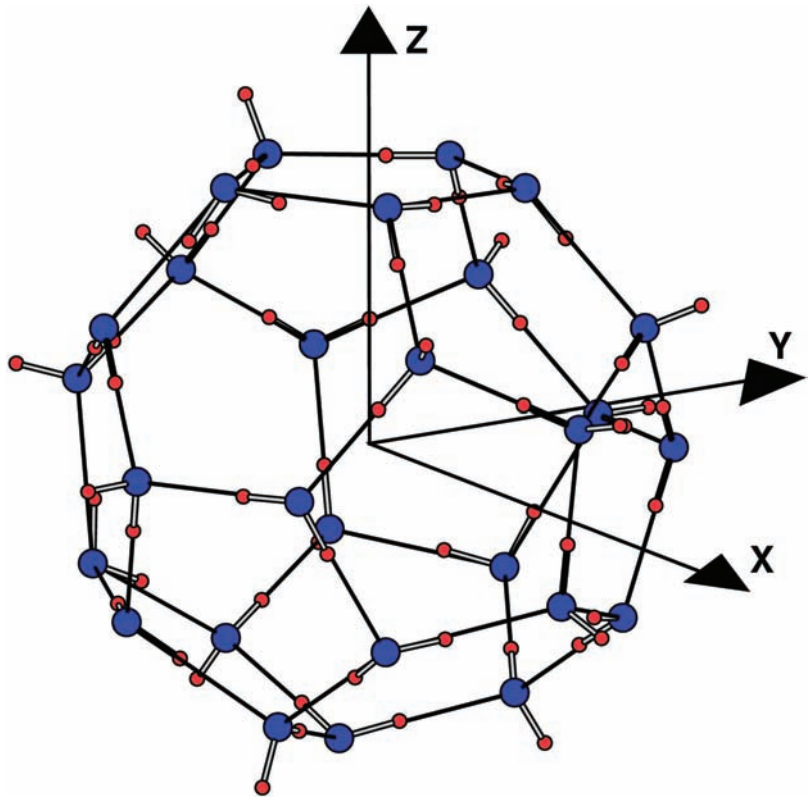

Figure 1. The geometry of the large hexakaidecahedral ($5^{12}6^4$) cage. The Cartesian *X*, *Y*, and *Z* axes coincide with the three principal axes of the cage, and their origin is at the center of mass of the cage.

II. Theory

A. Cage Geometry. The geometry of the large cage has been defined earlier.[22] The O atoms of the 28 water molecules forming the large cage occupy the corners of the hexakaidecahedron ($5^{12}6^4$) shown in Figure 1, which has 12 pentagonal and 4 hexagonal faces, in the positions determined by X-ray crystallography.[23] A hydrogen atom of a framework water molecule lies on each edge of the cage, linking by a hydrogen bond the two O atoms at the corners connected by the edge. The H atoms are configurationally disordered. The calculated number of distinct hydrogen-bonding (H−B) arrangements exceeds 30 000 for the small 5^{12} cage,[31] and is undoubtedly much greater for the large $5^{12}6^4$ cage. The one predominantly used in this work, displayed in Figure 1, was chosen at random with the goal of distributing the nonbonded O−H bonds evenly over the cage exterior. The quantum 5D calculations of the T-R energy levels were performed for several additional H−B topologies yielding virtually indistinguishable results.

B. Calculations of the Quantum Translation−Rotation Dynamics. The computational methodology for the calculation of the T-R energy levels of a single diatomic molecule in nanoconfinement was described previously.[17,21] The cage is treated as rigid, while the quantum 5D T-R dynamics of the guest molecule, which is also taken to be rigid, is treated rigorously, as fully coupled. The set of five coordinates (x,y,z,θ,ϕ) is employed; *x*, *y*, and *z* are the Cartesian coordinates of the cm of the hydrogen molecule, while the two polar angles θ and ϕ specify its orientation. The coordinate system is aligned with the principal axes of the cage, and its origin is at the cm of the cage. The computational scheme relies on the 3D direct-product discrete variable representation (DVR)[32,33] for the *x*, *y*, and *z* coordinates and the spherical harmonics for the angular θ and ϕ coordinates. The size of the final Hamiltonian matrix is drastically reduced by means of the sequential diagonalization and truncation procedure,[32,34,35] without loss of accuracy. Diagonalization of this truncated Hamiltonian matrix produces the 5D T-R energy levels and wave functions which are numerically exact for the potential energy surface (PES) employed. The dimension of the sine-DVR basis was 18 for each of the three Cartesian coordinates, and its grid spanned the range -5.1 au $\leq \lambda \leq 5.1$ au ($\lambda = x, y, z$). The angular basis included functions up to $j_{max} = 5$. The energy cutoff parameter for the intermediate 3D eigenvector basis[36] was set to 1080 cm^{-1} for H_2, and 880 cm^{-1} for HD and D_2, resulting in the final 5D Hamiltonian matrices of dimension 20 631 for H_2, 23 570 for HD, and 37 000 for D_2. These basis set parameters were tested extensively for convergence. The rotational constants used in our calculations were $B_{H_2} = 59.322$ cm^{-1}, $B_{HD} = 44.662$ cm^{-1}, and $B_{D_2} = 29.904$ cm^{-1}.

C. Potential Energy Surface: Large Cage vs. Small Cage. As in our past work on the hydrogen hydrates, the intermolecular interaction of the encapsulated hydrogen molecule with the water nanocage is assumed to be pairwise additive. Consequently, the 5D interaction potential V_{H_2-cage} between the confined H_2 molecule and *N* H_2O molecules forming the cage ($N = 28$ for the large cage) is written as

$$V_{H_2-cage}(q) = \sum_{w=1}^{N} V_{H_2-H_2O}(q, \Xi_w) \qquad (1)$$

where *q* are the coordinates (x,y,z,θ,ϕ) of the H_2 molecule defined above, $V_{H_2-H_2O}$ is the pair interaction specified below between H_2 and a framework H_2O molecule, and the index *w* runs over the water molecules of the cage, whose coordinates Ξ_w are fixed.

As mentioned in Section I, the 5D H_2−cage PES $V_{H_2-cage}(q)$ is based on the interaction potential by Alavi et al.,[29] and we denote it as SPC/E. The pair interaction $V_{H_2-H_2O}$ in eq 1

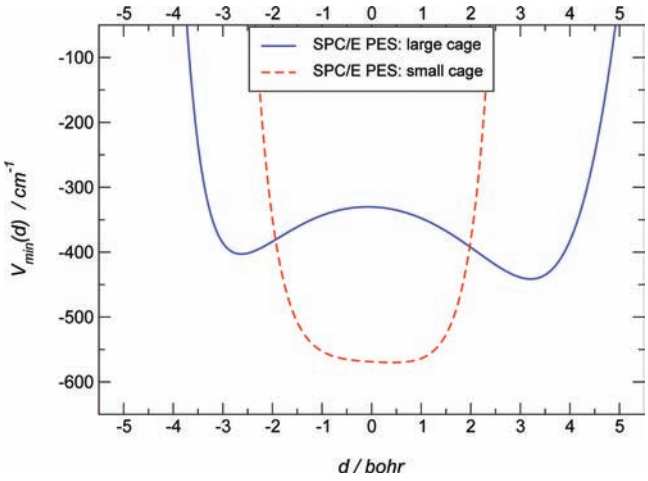

Figure 2. One-dimensional cuts through the 5D SPC/E PESs of H_2 in large and the small cages. The potential profiles shown are plotted along the lines that connect the global minima of the respective PESs with the center of the cages. Their slight asymmetry is caused by the configurational disorder of the H atoms of the framework water molecules.

combines the Coulomb interactions between the three point charges on the H_2O molecule, taken from the SPC/E effective pair potential model for water,[30] and the three point charges on the H_2 molecule chosen to reproduce its gas-phase quadrupole moment, with the Lennard-Jones interaction between the O atom of H_2O and the cm of H_2. The details can be found in our two recent papers.[21,22]

Figure 2 shows the potential profile of the SPC/E PES along the line that connects the global minimum of the PES with the center of the large cage. For comparison, the same 1D potential cut is shown through the SPC/E PES of the small dodecahedral cage used in ref 21. Clearly, the PESs of H_2 in the large and small cages are very different. The diameter of the cavity accessible to H_2 in the large cage is almost twice that of the small cage, giving the guest molecule much more room to move, or "rattle", at any given excitation energy. This fact alone suggests that the quantum T-R dynamics in the large cage is quantitatively, and possibly qualitatively, different from that in the small cage. In addition, while the PES of H_2 in the small cage is rather flat in the central region, the PES for H_2 inside the large cage has a maximum at the cage center with the energy of -330.31 cm^{-1}, lying $\sim$111 cm^{-1} above the off-center global minimum at -441.54 cm^{-1}.[22] The slight asymmetry of both potential cuts in Figure 2, especially evident for the large cage, arises from the inherently nonsymmetric H$-$B arrangement of the H atoms of the framework water molecules.

III. Results and Discussion

The lower lying purely translationally excited ($j = 0$) T-R energy levels of p-H_2, HD, and o-D_2 inside the large cage, from the quantum 5D calculations on the SPC/E PES, are given in Table 1. They are converged to 0.01 cm^{-1} or better. Therefore, the energy differences between the neighboring levels in Table 1, which in many instances are on the order of 0.1 cm^{-1}, are genuine, and not due to convergence error. For each state, the root-mean-square (rms) amplitudes Δx, Δy, and Δz are shown, which measure the wave function delocalization in the x-, y-, and z-directions, respectively, and can be helpful in making the quantum number assignments. The excitation energies ΔE in Table 1 are relative to the ground state energies of the encapsulated p-H_2 (-332.77 cm^{-1}), HD (-339.88 cm^{-1}), and o-D_2 (-345.12 cm^{-1}), respectively. Since the global minimum of the cage is at -441.54 cm^{-1}, the zero-point energy (ZPE) of the T-R motions is equal to 108.77 cm^{-1} for p-H_2, 101.66 cm^{-1} for HD, and 96.42 cm^{-1} for o-D_2. Interestingly. these ZPEs are just slightly smaller than the energy gap of 111 cm^{-1} between the potential maximum at the center of the cage and the off-center global minimum.

TABLE 1: One-, Two-, and Three-Quanta Translational ($j = 0$) Excitation Energies ΔE of p-H_2, HD, and o-D_2 in the Large Cage from the Quantum 5D Calculations on the SPC/E PES[a]

	p-H_2				HD	o-D_2
	ΔE	Δx	Δy	Δz	ΔE	ΔE
$n = 0, l = 0$	0.0	1.3 (0.6)	1.3 (0.6)	1.3 (0.6)	0.0	0.0
	16.4	1.1 (0.7)	1.8 (1.0)	1.1 (0.5)	10.4	6.9
$n = 1, l = 1$	16.5	1.1 (1.0)	1.1 (0.7)	1.8 (0.5)	10.5	7.1
	16.6	1.8 (0.6)	1.1 (0.6)	1.1 (0.9)	10.7	7.4
	39.2	1.3 (1.0)	1.5 (1.0)	1.5 (0.5)	25.4	17.5
	39.3	1.4 (1.0)	1.3 (1.0)	1.7 (0.5)	25.6	17.8
$n = 2, l = 2$	39.4	1.7 (0.9)	1.6 (0.9)	1.1 (0.6)	25.7	18.0
	45.2	1.6 (0.6)	1.5 (0.9)	1.2 (0.9)	30.5	22.3
	45.3	1.3 (0.9)	1.4 (0.6)	1.6 (0.9)	30.6	22.5
$n = 3, l = 3$	65.3	1.6	1.6	1.6		
$n = 2, l = 0$	72.8	1.2 (0.6)	1.2 (0.6)	1.2 (1.0)	54.1	45.2
	74.5	1.2	1.6	1.6		
	74.6	1.6	1.6	1.4		
	74.7	1.3	1.5	1.7		
$n = 3, l = 3$	74.7	1.6	1.6	1.4		
	74.8	1.7	1.4	1.5		
	74.8	1.6	1.4	1.6		
	110.9	1.3	1.6	1.1		
$n = 3, l = 1$	110.9	1.1	1.1	1.7		
	111.1	1.6	1.3	1.1		

[a] For p-H_2 only, the root-mean-square (rms) amplitudes Δx, Δy, and Δz (in bohr) are shown as well. The quantum numbers n and l are those of the 3D isotropic harmonic oscillator. The numbers in parentheses are the rms amplitudes of the corresponding one- and two-quanta translational excitations for H_2 in the small dodecahedral cage, from the quantum 5D calculations on the SPC/E PES in ref 21.

A. Translational Excitations: Quantum Numbers and Crystal Field Splittings. The first three excited T-R energy levels in Table 1, which are almost degenerate (16.4$-$16.6 cm^{-1} for p-H_2), correspond to the fundamental translational excitations of the caged molecule. This is evident from the plots of the translational components of these states displayed in Figure 3 for p-H_2, which have a single nodal plane each perpendicular to the y, z, and x axis, respectively, and also from the significantly larger rms amplitudes Δy, Δz, and Δx, respectively, relative to the corresponding ground state values. On the basis of the wave function plots in Figure 3, it would appear that the Cartesian quantum numbers $(\upsilon_x,\upsilon_y,\upsilon_z)$ can be used to assign the T-R eigenstates in the large cage. However, inspection of the higher lying T-R eigenstates of p-H_2, HD, and o-D_2 with two and three quanta in the translational modes listed in Table 1 reveals patterns which cannot be accounted for in a satisfactory manner with the Cartesian quantum number assignments. For example, of the six two-quanta excitations, five are clumped together (for p-H_2, they range from 39.2 to 45.3 cm^{-1}), while the sixth has a considerably higher energy (72.8 cm^{-1} for p-H_2). Likewise, the ten three-quanta excitations are split into two groups, consisting of seven and three closely spaced states, respectively; in the case of p-H_2, the group of seven states lies within the interval 65.3$-$74.8 cm^{-1}, while the other three

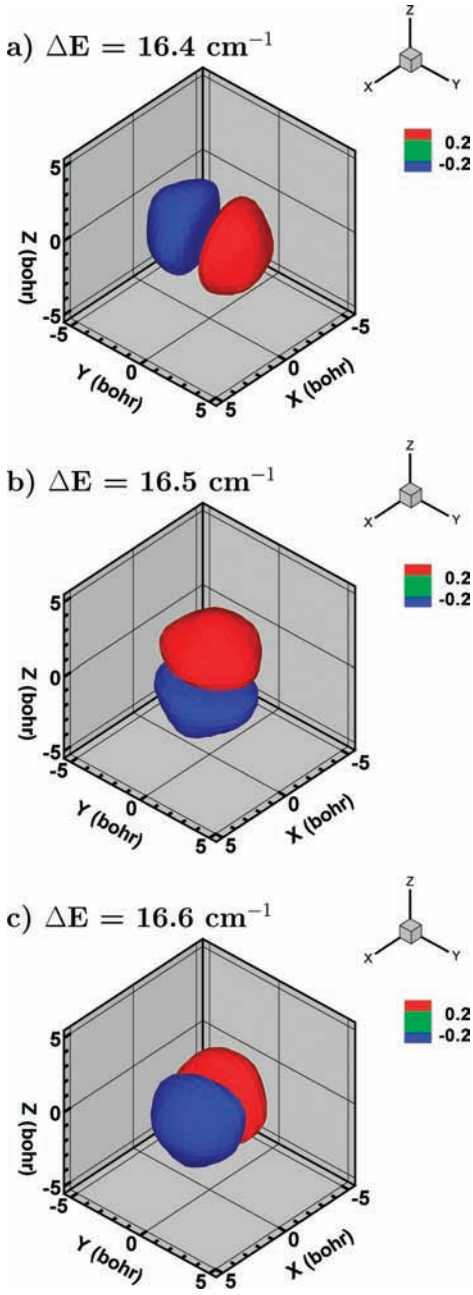

Figure 3. The 3D isosurfaces of the translational parts of the wave functions of the three $n = 1$, $l = 1$ states of p-H_2 in the large cage. These states, listed in Table 1, have one quantum of excitation in the translational modes. The excitation energies ΔE are relative to the ground state.

states are nearly degenerate, at 110.9−111.1 cm^{-1}. The inadequacy of the Cartesian quantum numbers is reinforced by the wave function plots of the two-quanta states for p-H_2 shown in Figure 4.

A natural and simple explanation for both the energy level patterns and the translational wave function plots in Figure 4 is provided by the physical picture where, for the purpose of assignment only, the translational modes are viewed as those of the 3D isotropic harmonic oscillator (HO). The energy levels of the 3D isotropic HO are labeled by the principal quantum number n and the orbital angular momentum quantum number l, whose allowed values are n, $n - 2$, ..., 1 or 0, for odd or even n, respectively.[37] When the possible values of m, $-l \le m \le l$, are taken into account, the degree of degeneracy of the energy levels of the isotropic 3D HO is $^1/_2(n + 1)(n + 2)$, e.g., 3 for $n = 1$, 6 for $n = 2$, and 10 for $n = 3$.

In this picture, the five closely spaced two-quanta excitations appearing in Table 1 are understood to represent the $n = 2$, $l = 2$ quintuplet, while the sixth, whose energy is significantly higher, is the single $n = 2$, $l = 0$ state. This assignment is supported by the wave function plots displayed in Figure 4. In the same vein, the two manifolds with seven and three three-quanta states are assigned as $n = 3$, $l = 3$ and $n = 3$, $l = 1$, respectively. These quantum number assignments are given in Table 1.

It should be emphasized that although the model of the 3D isotropic HO and its quantum numbers is successful in correlating and assigning the T-R levels in the large cage, the translationally excited states are definitely *not* harmonic. As Table 1 shows, their energies depend not only on n, as in the true 3D isotropic HO,[37] but also quite strongly on l, evidence of their pronounced *anharmonicity*. For example, the energy difference between the $n = 2$, $l = 0$ level and the highest level with $n = 2$, $l = 2$ is 27.5 cm^{-1} for p-H_2, 23.5 cm^{-1} for HD, and 22.7 cm^{-1} for o-D_2. We found the same behavior for the calculated T-R levels of H_2, HD, and D_2 in C_{60}.[38,39] The anharmonicity of the translational modes is evident also from the ratio of the translational fundamentals for p-H_2 (∼16.5 cm^{-1}) and o-D_2 (∼7.1 cm^{-1}), which is ∼2.3, very different from $2^{1/2} \approx 1.414$ in the HO limit.

The T-R energy levels of p-H_2, HD, and o-D_2 with $l > 1$ in Table 1 exhibit another intriguing feature, which is not explained by the 3D isotropic HO model alone. The five $n = 2$, $l = 2$ levels are clearly split into two groups, having three and two nearly degenerate levels, respectively (for p-H_2, 39.2−39.4 and 45.2−45.3 cm^{-1}). We believe that this splitting, about 6 cm^{-1} in the case of p-H_2 (5 cm^{-1} for HD and 4.5 cm^{-1} for o-D_2), is caused by the "crystal field" of the large cage, since it matches the group-theoretical prediction regarding the levels with $l = 2$. If only the positions of the O atoms are considered, the large hexakaidecahedral cage has T_d symmetry. Group theory[40] shows that in the environment of T_d symmetry, $l = 2$ levels are split into a triply degenerate set of states and a doubly degenerate set [which belong to T_2 and E irreducible representations (IRs), respectively]. The configurational disorder of the H atoms of the framework water molecules lowers the symmetry of the large cage, but the symmetry of the environment of the guest hydrogen molecule evidently remains essentially T_d. The disordered arrangement of the H atoms is likely to be responsible for the fact that the $l = 2$ levels within each of the two sets are not exactly degenerate.

As for the seven $n = 3$, $l = 3$ levels of p-H_2 in Table 1, one of them, at 65.3 cm^{-1}, lies ∼9.4 cm^{-1} below the other six closely spaced levels at 74.5−74.8 cm^{-1}. This is in good agreement with the group theory, which predicts that in T_d environment the levels with $l = 3$ should be split into one nondegenerate state and two triply degenerate sets of states (IRs $A_2 + T_1 + T_2$).[40] That the two triply degenerate sets of states actually appear as a single group of six states is probably due to the weak "crystal field" splitting of the two sets, and also to the configurational disorder of the H atoms.

The $l = 1$ levels should be left unsplit in the environment of T_d symmetry,[40] and this is indeed the case with the $n = 1$, $l = 1$ levels listed in Table 1.

Crystal-field splitting of certain T-R energy levels was observed also in our quantum 5D calculations of H_2, HD, and D_2 in C_{60},[38,39] in accordance with the group-theory rules for the icosahedral I_h environment of the fullerene cage.[41] However,

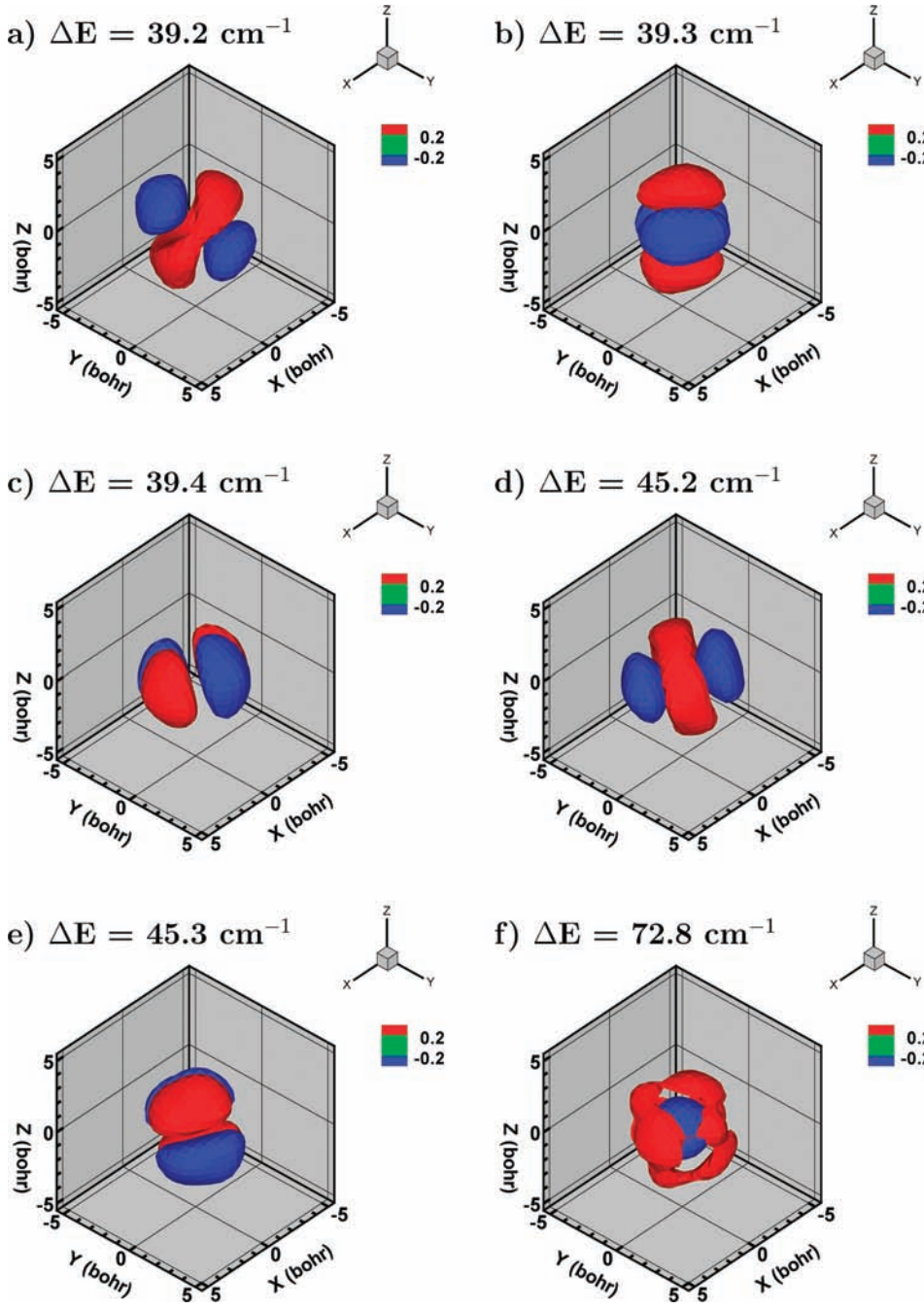

Figure 4. The 3D isosurfaces of the translational parts of the wave functions of the six $n = 2$ states of p-H_2 in the large cage. These states, listed in Table 1, have two quanta of excitation in the translational modes. Panels a−e show the wave function of the five $n = 2$, $l = 2$ states, while panel f shows the wave function of the $n = 2$, $l = 0$ state. The excitation energies ΔE are relative to the ground state.

the level splittings induced by the nonsphericity of C_{60} are less than 1 cm^{-1}, much smaller than the splittings in the large cage of the sII clathrate hydrate, 5−10 cm^{-1}, reported in this paper.

It is interesting, and illuminating, to compare the qualitative and quantitative features of the translational excitations of p-H_2, HD, and o-D_2 inside the large cage with those in the small cage, which we investigated recently.[21] While the quantum numbers n and l of the 3D isotropic HO are used in this work to assign the T-R energy levels in the large cage, the translational excitations in the small cage have been assigned in terms of the quantum numbers v and l (actually $|l|$) of the 2D isotropic HO for the in-plane (xy) modes, and the Cartesian quantum number v_z for the perpendicular z-mode excitations.[21] This difference in the quantum numbers implies that the environment of the small cage is somewhat less symmetric than that of the large cage. To shed some light on this, we calculated the three principal moments of inertia, and the corresponding rotational constants, of the large and small cages, by first taking into account only the O atoms. For the large cage, all three rotational constants turned out to be identical, 2.576 × 10^{-3} cm^{-1}, while for the small cage, two rotational constants are the same, 5.261 × 10^{-3} cm^{-1}, and the third one is smaller, 5.063 × 10^{-3} cm^{-1} (inclusion of the water H atoms causes very small changes of these numbers). Hence, the large cage is essentially a spherical top, and the small cage has the lower symmetry of a (slightly) oblate symmetric top. These findings correlate extremely well with the two sets of translational quantum numbers used for the large and small cages, respectively. In addition, the fact that the small cage is an oblate (and not a prolate) symmetric top is fully consistent with our quantum 5D results for p-H_2 in the

TABLE 2: The $j = 0 \rightarrow 1$ and $j = 0 \rightarrow 2$ Rotational Excitation Energies (in cm^{-1}) of H_2, HD, and D_2 in the Large Cage, for the Translational Ground State, from the Quantum 5D Calculations on the SPC/E PES[a]

	H_2		HD		D_2	
$j = 1$		110.7		83.9		51.3
	[118.6]	116.4	[89.3]	87.8	[59.8]	57.3
		129.2		98.6		68.3
Δ		18.5		14.7		17.0
		(19.1)		(13.0)		(19.1)
$j = 2$		349.1				
		349.6				
	[355.9]	356.7				
		360.1				
		361.8				
Δ		12.7				
		(15.7)				

[a] The excitation energies are relative to the ground state energies E_0 of p-H_2 (−332.77 cm^{-1}), HD (−339.88 cm^{-1}), and o-D_2 (−345.12 cm^{-1}), respectively. Δ denotes the splittings of the $j = 1$ triplet and $j = 2$ quintuplet in the large cage. The energies in square brackets are the $j = 1$ and 2 rotational levels of H_2, HD, and D_2, respectively, in the gas phase. The numbers in parentheses are the corresponding $j = 1$ and 2 splittings, respectively, calculated on the SPC/E PES for H_2, HD, and D_2 in the small dodecahedral cage, from ref 21.

small cage[21] showing that the frequency of the 2D in-plane (xy) mode fundamental, 74.6 cm^{-1}, is lower than the frequency of the z-mode fundamental, 97.5 cm^{-1}.

Besides these qualitative differences, there are also quantitative differences between the translational excitations of the guest molecule in the large and small cages. For all three isotopomers, the frequency of the translational fundamental inside the large cage is much lower than those in the small cage. Thus, for p-H_2, the translational fundamental in the large cage (16.5 cm^{-1}) is smaller than those of the 2D xy-mode (74.6 cm^{-1}) and the z-mode (97.5 cm^{-1}) fundamentals in the small cage[21] by the factor of 4.5 to 6, respectively. This factor is even larger in the case of o-D_2, 6.5 to 8.7. The reason for this difference is clear from Figure 2; it shows that the diameter of the large cage is roughly twice that of the small cage, which gives the trapped molecule significantly more room to move and results in much lower frequencies of the translational fundamental and the higher translational excitations. The greater freedom of motion of the guest molecule inside the large cage is evident also from the comparison of the rms amplitudes Δx, Δy, and Δz for p-H_2 in the large and small cages shown in Table 1. For all the excitations considered, the rms amplitudes are typically 50−100% bigger in the large cage than in the small one.

B. Rotational Excitations and Comparison with Raman Spectroscopy. So far, we have discussed only the translational excitations of the hydrogen molecule (in the ground rotational state) inside the large cage, and how they compare to those in the small cage. We now turn our attention to the purely rotational excitations of H_2, HD, and D_2 in the large cage shown in Table 2, when the guest molecules are in the ground translational state. The $2j + 1$ degeneracy of the $j = 1$ and 2 levels is completely lifted due to the angular anisotropy of the H_2−cage PES, very similar to what we found for these molecules in the small cage.[21] The $j = 1$ triplet is split into three distinct levels, one of which is close in energy to the (triply degenerate) $j = 1$ level in the gas phase, while the other two lie below and above the central level, respectively. The splitting of the $j = 1$ triplet shows rather weak isotopomer dependence, ranging from 18.5 cm^{-1} for H_2 to 14.7 cm^{-1} for HD. The $j = 2$ quintuplet has one level in the center of the pattern, virtually unshifted from the (5-fold degenerate) $j = 2$ level of the gas-phase molecule, and the other four are grouped into two pairs of closely spaced levels separated by ∼1 cm^{-1}, one pair lying energetically above and the other below the central component. The $j = 2$ levels are shown in Table 2 for H_2 only, since the greater density of states of HD and D_2 makes the unambiguous identification of the $j = 2$ states which are in the translational ground state considerably more problematic.

The splittings of the $j = 1$ and 2 multiplets in the large cage resemble very closely the corresponding splittings which we have calculated for the small cage,[21] both in terms of their patterns, which are nearly identical, and also their magnitudes, as well as the energies of the individual components. The implication is that the angular, or orientational, anisotropies of the environment experienced by a hydrogen molecule in the large and small cages are comparable, despite the fact that the two cages differ greatly in size. The large-cage splittings of the $j = 1$ triplet of H_2, HD, and D_2 are within 1−2 cm^{-1} of those in the small cage, and the splitting of the $j = 2$ quintuplet of p-H_2 in the large cage is about 3 cm^{-1} smaller than in the small cage. On the basis of this, one would expect the $S_0(0)$ ($j = 0 \rightarrow 2$) bands for large and small cages to be very similar in their appearance and frequencies, and that the rotational band for the large cage should be slightly narrower than that for the small cage.

These expectations are entirely borne out by the measured rotational Raman spectra for simple H_2 and binary THF + H_2 sII clathrate hydrates.[26,27] As mentioned in the Introduction, the $S_0(0)$ bands of simple H_2 hydrate, where H_2 occupies both the large and small cages, and THF + H_2 hydrate, in which only the small cages are (singly) occupied by H_2 (THF occupies the large cages), do exhibit remarkable similarity with respect to their frequencies, widths, and shapes, when the H_2 occupancy of the large cage is low, less than three molecules; see Figure 9 in ref 27. Moreover, the $S_0(0)$ band of simple H_2 hydrate is indeed a bit narrower than the same band for THF + H_2 hydrate.

The striking similarity between the $S_0(0)$ bands of simple H_2 hydrate and THF + H_2 hydrate extends to the three distinct peaks at their top, which are about 3.5 cm^{-1} apart in the former and slightly more (∼4 cm^{-1}) in the latter.[27] It is virtually certain that the two outer peaks to the red and blue, respectively, of the peak at the center of the $S_0(0)$ band arise from the transitions to the two closely spaced pairs of states of the computed $j = 2$ quintuplet, energetically below and above the central state, which are not resolved in the Raman spectra of either hydrate.

The $S_0(1)$ ($j = 1 \rightarrow 3$) bands measured for simple H_2 hydrate and THF + H_2 hydrate also show a high degree of similarity, when the H_2 content of the large cage is low.[27] The explanation for this is the same as in the case of the $S_0(0)$ bands above: the magnitudes and patterns of the splittings of the initial and final levels of this rotational transition in the large and small cages are comparable for low H_2 occupancy of the former. Moreover, the $j = 1$ and 3 levels are split into three and seven components, respectively, allowing for numerous rotational transitions differing very little in energy, which may be hard to resolve experimentally. This would account for the apparent lack of structure in the measured $S_0(1)$ bands, which appear as broad, nearly symmetric peaks.[26,27]

The overall agreement between theory and experiment regarding the $j = 0 \rightarrow 2$ transitions in the large cage is very good. A more quantitative comparison reveals that the energy of the central component of the $j = 2$ quintuplet computed for H_2 inside the large cage, 356.7 cm^{-1} (Table 2), is ∼6 cm^{-1} higher than

that of the central peak of the measured $S_0(0)$ band[27] at ~351 cm^{-1}. As a result, the entire calculated $j = 2$ quintuplet is shifted by about 6 cm^{-1} relative to the $S_0(0)$ band measured for simple H_2 hydrate at low H_2 loading of the large cavity, and its width (splitting) is slightly greater. This is best seen in Figure 10 of ref 27; the comparison there is made for H_2 (and D_2) in the small cage of THF + H_2 hydrate, but it is relevant in view of the great similarity of the rotational excitations in the small and large cages (at the low H_2 occupancy of the latter). We believe that the main reason for the above ~6 cm^{-1} discrepancy is the use of the gas-phase rotational constant for H_2, $B_{H_2} = 59.322$ cm^{-1}, in our quantum 5D calculations. The calculated energy of the state at the center of the $j = 2$ quintuplet, 356.7 cm^{-1}, is very close to the gas-phase value of $6B_{H_2} = 355.9$ cm^{-1}. Inclusion of the centrifugal distortion using the gas-phase value of the distortion constant, 0.0471 cm^{-1}, would decrease the energy of the central peak by about 1.7 cm^{-1}. This would bring it, and the entire computed $j = 2$ quintuplet, into slightly better agreement with the observed $S_0(0)$ band, but not enough to eliminate the difference. The energy of the central peak of the experimental $S_0(0)$ band would remain several wave numbers lower, implying that the *effective* (vibrationally averaged) rotational constant of the confined H_2 molecule is *slightly smaller* than that in the gas phase, as a result of the H_2−cage interactions which soften the *intra*molecular potential of H_2. The recent infrared spectroscopic study[42] of the endohedral complex $H_2@C_{60}$ found a comparable reduction in the effective rotational constant of H_2, from 59.322 (gas phase) to 57.8 cm^{-1}. A first-principles determination of the effective rotational constant of H_2 in the clathrate hydrate cages would require a high-level ab initio electronic structure calculation of the 6D interaction potential between a flexible H_2 molecule and the rigid cage (small or large), an exceedingly time-consuming computational task.

In the closing of this section we point to another feature of the rotational Raman spectra of the hydrogen hydrates which conforms to our theoretical predictions. The $S_0(0)$ bands measured for THF + H_2 and THF + D_2 hydrates (in which the H_2/D_2 molecule is restricted to the small cages) have virtually identical shapes, widths, and spacing between the three peaks which they exhibit.[27] This is in agreement with our earlier quantum 5D results for H_2 and D_2 in the small cage,[21] which showed that the splittings of the $j = 0 \rightarrow 2$ transitions, as well as the separation between the two closely spaced doublets and the central component of the quintuplet, are practically the same for H_2 and D_2; see Table 7 in ref 21 and also Figure 10 of ref 27. There is little doubt that the same holds for the hydrogen molecule isotopomers confined in the large cage.

IV. Conclusions

We have reported rigorous quantum 5D calculations of the T-R energy levels and wave functions of a single H_2, HD, and D_2 molecule inside the large hexakaidecahedral ($5^{12}6^4$) cage of the sII clathrate hydrate. The SPC/E PES of Alavi and co-workers[29] was used in the calculations. The energy range of well-converged eigenstates extends beyond the $j = 2$ rotational levels of the guest molecules. Inspection of the calculated T-R energy level structure and the translational components of the wave functions showed that the quantum numbers appropriate for assigning the translationally excited levels are the principal quantum number n and the orbital angular momentum quantum number l of the 3D isotropic harmonic oscillator (HO). The translational ($j = 0$) states with up to three quanta of excitation have been assigned in this manner. Although the quantum numbers n and l of the 3D isotropic HO are successful in organizing and understanding the patterns of the T-R energy levels, the translationally excited states are far from harmonic. In addition to n, their energies depend strongly on l, which is not the case with the 3D isotropic HO.

When l is greater than one, the T-R levels with the same n and l are split into groups of almost degenerate levels. The patterns of these splittings for $l = 2$ and 3 are in accordance with the predictions of group theory regarding the "crystal field" splittings in the environment of T_d symmetry. If only the O atoms are taken into account, the large cage belongs to the T_d point group, and the interior of the cage evidently retains this symmetry to a high degree despite the configurational disorder of the H atoms of the framework water molecules. The crystal-field splittings in the large cage are substantial, about 6 cm^{-1} for the $n = 2$, $l = 2$ levels of p-H_2, and ~9 cm^{-1} for $n = 3$, $l = 3$. They are much larger than the T-R level splittings of less than 1 cm^{-1} found in our quantum 5D calculations of $H_2@C_{60}$,[38,39] which are induced by the icosahedral I_h environment of the fullerene cage.

The frequencies of the translational fundamentals of H_2, HD, and D_2 inside the large cage are much lower (by a factor of 4.5−6 for H_2 and 6.5−8.7 for D_2) than those in the small cage calculated by us recently.[21] This is primarily due to the fact that the diameter of the large cage is almost twice that of the small cage, giving the guest molecule significantly more room to move.

The angular anisotropy of the H_2−cage interaction potential removes completely the $2j + 1$ degeneracy of the $j = 1$ and 2 rotational levels of the hydrogen molecule confined inside the large cage. The patterns and magnitudes of the splittings of the $j = 1$ and 2 multiplets in the large cage, as well as the energies of the sublevels, are nearly identical with those computed for the small cage.[21] This would lead one to expect that the $S_0(0)$ ($j = 0 \rightarrow 2$) bands for the large and small cages should have very similar shapes and frequencies. Indeed, the $S_0(0)$ bands in the rotational Raman spectra measured for simple H_2 hydrate and THF + H_2 hydrate are strikingly similar in their frequencies, widths, shapes, and internal structure, when the H_2 occupancy of the large cage of simple H_2 hydrate is low.[27] Both rotational bands have three distinguishable peaks; the two outer peaks can be attributed to the two closely spaced pairs of states lying below and above the central component, respectively, of the $j = 2$ quintuplet calculated for both the small and large cages, which have not been resolved in the Raman spectra.

We are currently working on several theoretical approaches for calculating accurately the excited T-R energy levels when the large cage is occupied by multiple H_2 molecules. One of the challenges that these methodological developments will tackle is understanding quantitatively the origin of the observed substantial broadening of the $S_0(0)$ band for simple H_2 hydrate with the increasing H_2 occupancy of the large cage. The calculations presented in this paper constitute the requisite first step in this direction.

Acknowledgment. Z.B. is grateful to the National Science Foundation for partial support of this research, through Grant CHE-0315508. The computational resources used in this work were funded in part by NSF MRI grant CHE-0420870. Acknowledgment is made to the donors of the American Chemical Society Petroleum Research Fund for partial support of this research. We thank the reviewers for their constructive comments.

References and Notes

(1) Mao, W. L.; Koh, C. A.; Sloan, E. D. *Phys. Today* **2007**, *42* (10), 60.

(2) Struzhkin, V. V.; Militzer, B.; Mao, W. L.; Mao, H. K.; Hemley, R. J. *Chem. Rev.* **2007**, *107*, 4133.

(3) Sloan, E. D. *Clathrate hydrates of natural gases*; Marcel Dekker: New York, 1998.

(4) Dyadin, Y. A.; Larionov, E. G.; Manakov, A. Y.; Zhurko, F. V.; Aladko, E. Y.; Mikina, T. V.; Komarov, V. Y. *Mendeleev Commun.* **1999**, *9*, 209.

(5) Mao, W. L.; Mao, H. K.; Goncharov, A. F.; Struzhkin, V. V.; Guo, Q.; Hu, J.; Shu, J.; Hemley, R. J.; Somayazulu, M.; Zhao, Y. *Science* **2002**, *297*, 2247.

(6) Lokshin, K. A.; Zhao, Y.; He, D.; Mao, W. L.; Mao, H. K.; Hemley, R. J.; Lobanov, M. V.; Greenblatt, M. *Phys. Rev. Lett.* **2004**, *93*, 125503.

(7) Mao, W. L.; Mao, H. K. *Proc. Natl. Acad. Sci. U.S.A.* **2004**, *101*, 708.

(8) Schüth, F. *Nature* **2005**, *434*, 712.

(9) Hu, Y. H.; Ruckenstein, E. *Angew. Chem., Int. Ed.* **2006**, *45*, 2011.

(10) Florusse, L. J.; Peters, C. J.; Schoonman, J.; Hester, K. C.; Koh, C. A.; Dec, S. F.; Marsh, K. N.; Sloan, E. D. *Science* **2004**, *306*, 469.

(11) Lee, H.; Lee, J.-W.; Kim, D. Y.; Park, J.; Seo, Y.-T.; Zeng, H.; Moudrakovski, I. L.; Ratcliffe, C. J.; Ripmeester, J. A. *Nature* **2005**, *434*, 743.

(12) Kim, D. Y.; Lee, H. *J. Am. Chem. Soc.* **2005**, *127*, 9996.

(13) Strobel, T. A.; Koh, C. A.; Sloan, E. D. *J. Phys. Chem. B* **2008**, *112*, 1185.

(14) Patchkovskii, S.; Tse, J. S. *Proc. Natl. Acad. Sci. U.S.A.* **2003**, *100*, 14645.

(15) Patchkovskii, S.; Yurchenko, S. N. *Phys. Chem. Chem. Phys.* **2004**, *6*, 4152.

(16) Inerbaev, T. M.; Belosludov, V. R.; Belosludov, R. V.; Sluiter, M.; Kawazoe, Y. *Comput. Mater. Sci.* **2006**, *36*, 229.

(17) Xu, M.; Elmatad, Y.; Sebastianelli, F.; Moskowitz, J. W.; Bačić, Z. *J. Phys. Chem. B* **2006**, *110*, 24806.

(18) Sebastianelli, F.; Xu, M.; Elmatad, Y.; Moskowitz, J. W.; Bačić, Z. *J. Phys. Chem. C* **2007**, *111*, 2497.

(19) Sebastianelli, F.; Xu, M.; Kanan, D. K.; Bačić, Z. *J. Phys. Chem. A* **2007**, *111*, 6115.

(20) Xu, M.; Sebastianelli, F.; Bačić, Z. *J. Phys. Chem. A* **2007**, *111*, 12763.

(21) Xu, M.; Sebastianelli, F.; Bačić, Z. *J. Chem. Phys.* **2008**, *128*, 244715.

(22) Sebastianelli, F.; Xu, M.; Bačić, Z. *J. Chem. Phys.* **2008**, *129*, 244706.

(23) Mak, T. C. W.; McMullan, R. K. *J. Chem. Phys.* **1965**, *42*, 2732.

(24) Ulivi, L.; Celli, M.; Gianassi, A.; Ramirez-Cuesta, A. J.; Bull, D. J.; Zoppi, M. *Phys. Rev. B* **2007**, *76*, 161401.

(25) Ulivi, L.; Celli, M.; Gianassi, A.; Ramirez-Cuesta, A. J.; Zoppi, M. *J. Phys.: Condens. Matter* **2008**, *20*, 104242.

(26) Gianassi, A.; Celli, M.; Ulivi, L.; Zoppi, M. *J. Chem. Phys.* **2008**, *129*, 084705.

(27) Strobel, T. A.; Sloan, E. D.; Koh, C. A. *J. Chem. Phys.* **2009**, *130*, 014506.

(28) Hodges, M. P.; Wheatley, R. J.; Schenter, G. K.; Harvey, A. H. *J. Chem. Phys.* **2004**, *120*, 710.

(29) Alavi, S.; Ripmeester, J. A.; Klug, D. D. *J. Chem. Phys.* **2005**, *123*, 024507.

(30) Berendsen, H. J. C.; Grigera, J. R.; Straatsma, T. P. *J. Phys. Chem.* **1987**, *91*, 6269.

(31) McDonald, S.; Ojamäe, L.; Singer, S. J. *J. Phys. Chem. A* **1998**, *102*, 2824.

(32) Bačić, Z.; Light, J. C. *Annu. Rev. Phys. Chem.* **1989**, *40*, 469.

(33) Mandziuk, M.; Bačić, Z. *J. Chem. Phys.* **1993**, *98*, 7165.

(34) Bačić, Z.; Light, J. C. *J. Chem. Phys.* **1986**, *85*, 4594.

(35) Bačić, Z.; Light, J. C. *J. Chem. Phys.* **1987**, *86*, 3065.

(36) Liu, S.; Bačić, Z.; Moskowitz, J. W.; Schmidt, K. E. *J. Chem. Phys.* **1995**, *103*, 1829.

(37) Landau, L. D.; Lifshitz, E. M., *Quantum Mechanics*; Pergamon Press: Oxford, UK, 1977.

(38) Xu, M.; Sebastianelli, F.; Bačić, Z.; Lawler, R.; Turro, N. J. *J. Chem. Phys.* **2008**, *128*, 011101.

(39) Xu, M.; Sebastianelli, F.; Bačić, Z.; Lawler, R.; Turro, N. J. *J. Chem. Phys.* **2008**, *129*, 064313.

(40) Cotton, F. A. *Chemical Application of Group Theory*, 2nd ed.; Wiley-Interscience: New York, 1970.

(41) Judd, B. R. *Proc. R. Soc. A* **1957**, *241*, 122.

(42) Mamone, S.; Ge, M.; Hüvonen, D.; Nagel, U.; Danquigny, A.; Cuda, F.; Grossel, M. C.; Murata, Y.; Komatsu, K.; Levitt, M. H.; Room, T.; Carravetta, M. *J. Chem. Phys.* **2009**, *130*, 081103.

JP901951K